2013

Comparison of Post-Detonation Combustion in Explosives Incorporating Aluminum Nanoparticles: Influence of the Passivation Layer

William K. Lewis
Air Force Research Laboratory

C. G. Rumchik
Air Force Research Laboratory

M. J. Smith
Air Force Research Laboratory

K. A. Shiral Fernando
University of Dayton, kfernando1@udayton.edu

Christopher A. Crouse
Air Force Research Laboratory

See next page for additional authors

Comparison of post-detonation combustion in explosives incorporating aluminum nanoparticles: Influence of the passivation layer

W. K. Lewis,[1,a)] C. G. Rumchik,[2] M. J. Smith,[3] K. A. S. Fernando,[1] C. A. Crouse,[4,5] J. E. Spowart,[4] E. A. Guliants,[1] and C. E. Bunker[3]
[1]*University of Dayton Research Institute, Dayton, Ohio 45469, USA*
[2]*U.S. Air Force Research Laboratory, Munitions Directorate, Eglin AFB, Florida 32542, USA*
[3]*U.S. Air Force Research Laboratory, Propulsion Directorate, Wright-Patterson AFB, Ohio 45433, USA*
[4]*U.S. Air Force Research Laboratory, Materials & Manufacturing Directorate, Wright-Patterson AFB, Ohio 45433, USA*
[5]*UES, Inc., Dayton, Ohio 45432, USA*

(Received 7 December 2012; accepted 17 January 2013; published online 31 January 2013)

Aluminum nanoparticles and explosive formulations that incorporate them have been a subject of ongoing interest due to the potential of aluminum particles to dramatically increase energy content relative to conventional organic explosives. We have used time-resolved atomic and molecular emission spectroscopy to monitor the combustion of aluminum nanoparticles within the overall chemical dynamics of post-detonation fireballs. We have studied the energy release dynamics of hexahydro-1,3,5-trinitro-1,3,5-triazine (RDX) charges incorporating three types of aluminum nanoparticles: commercial oxide-passivated nanoparticles, oleic acid-capped aluminum nanoparticles (AlOA), and nanoparticles in which the oxide shell of the particle has been functionalized with an acrylic monomer and copolymerized into a fluorinated acrylic matrix (AlFA). The results indicate that the commercial nanoparticles and the AlFA nanoparticles are oxidized at a similar rate, while the AlOA nanoparticles combust more quickly. This is most likely due to the fact that the commercial nano-Al and the AlFA particles are both oxide-passivated, while the AlOA particles are protected by an organic shell that is more easily compromised than an oxide layer. The peak fireball temperatures for RDX charges containing 20 wt. % of commercial nano-Al, AlFA, or AlOA were ~3900 K, ~3400 K, and ~4500 K, respectively. © *2013 American Institute of Physics*. [http://dx.doi.org/10.1063/1.4790159]

I. INTRODUCTION

Aluminum nanoparticles and explosive formulations that incorporate them have been a subject of significant interest in recent years due to the potential of aluminum particles to dramatically increase energy content relative to conventional organic explosives. To date, a large number of aluminized explosive formulations have been studied, as summarized in several reviews.[1,2] In general, it has been found that oxide-passivated aluminum nanoparticles particles react slowly relative to detonation processes and contribute primarily to "late-time effects" such as post-detonation fireball combustion and air blast[1] due to the high melting point[3] (2054 °C) and mechanical strength of the oxide shell that protects the aluminum metal core from oxidation. Since the properties of the passivation layer are thought to exert an important influence on the post-detonation chemistry, it seems reasonable to suspect that changing the nature of this layer might significantly influence the chemical dynamics.

In recent years, synthesis methods have been developed to produce aluminum nanoparticles which are passivated by an organic layer[4,5] rather the traditional oxide shell. Alternatively, synthesis routes to particles in which a pre-existing oxide layer is functionalized with various organic species have also been discovered.[6,7] We have previously synthesized[5] aluminum nanoparticles capped with oleic acid and characterized their reactivity.[8,9] In these particles, the organic shell is lost at temperatures of 200–300 °C, exposing the reactive core. These particles have also exhibited significantly enhanced reactivity with room temperature water,[8] as well as with ammonium nitrate and ammonium perchlorate matrices and their decomposition products after heating.[9]

The purpose of the current investigation is to study the post-detonation combustion dynamics of hexahydro-1,3,5-trinitro-1,3,5-triazine (RDX) charges incorporating three types of aluminum nanoparticles: commercial oxide-passivated nanoparticles, the oleic acid-capped aluminum nanoparticles (AlOA), and nanoparticles in which the pre-existing oxide shell of the aluminum particle has been functionalized[7] with an acrylic monomer and copolymerized in the presence of a fluorinated acrylate to yield an aluminum-fluorinated acrylic composite material (AlFA). The fluorocarbons in this material have been shown to vigorously react with the Al metal to produce AlF_3 and Al_4C_3 once ignited.[7] Reaction with O_2 in the surrounding air to produce Al_2O_3 also occurs (the material is fuel-rich), but the fluorination reaction is kinetically dominant, making this an intriguing candidate to also study in explosive formulations.

The progress of the post-detonation chemistry is tracked using atomic and molecular emission spectroscopy methods.

[a)]Author to whom correspondence should be addressed. Electronic mail: wlewis2@udayton.edu.

Temperatures are obtained using a previously developed atomic emission spectroscopy-based technique[10,11] which involves doping the explosive charge with an inorganic impurity. The temperature is then determined by monitoring the relative intensities of atomic emission lines corresponding to emission from different energy levels of a selected atom. Chemical dynamics are tracked via the time-dependent intensities of electronic emissions from species of interest, such as Al atomic lines and AlO vibronic bands. By combining temperature measurements with the time-resolved emission spectroscopy methods used by earlier groundbreaking investigations[12–18] to characterize the complex chemical dynamics occurring after the detonation of an explosive charge, we are able to monitor the combustion of aluminum particles within the overall chemical dynamics of the explosion and correlate this with the energy release process. We have successfully used this approach to study RDX charges incorporating nano- and micron-sized aluminum particles previously.[11]

II. EXPERIMENT

Pressed right-cylindrical charges (25 mm height × 25 mm diameter) of 20 g total mass were prepared from a mixture of RDX (73 wt. %), a hydroxyl-terminated polybutadiene (HTPB) binder (6 wt. %), and an aluminum powder (20 wt. %) chosen from commercial nano-Al, AlOA, or AlFA. In order to obtain temperature measurements during the post-detonation combustion via atomic emission spectroscopy, 1 wt. % ball-milled barium nitrate was added to the mixture and mixed thoroughly before pressing. Oxide-passivated nanoparticles (30–70 nm particle size) were obtained from Nano Technologies; the AlOA (20–70 nm particle sizes) and AlFA samples were synthesized as reported previously.[5,7] The AlFA material consisted of micron–sized particles containing oxide-passivated aluminum nanoparticles (30–130 nm size) polymerized into a fluorinated acrylic matrix. We note that the commercial nano-Al is ~80 wt. % active Al metal content. The AlOA particles are ~40 wt. % active Al; the AlFA particles are ~50 wt. % active Al. All charges were initiated using Reynolds RP-80 detonators placed on the end of each cylindrical charge.

Light from the explosions was collected from the end of the charge opposite the detonator using a 5 mm diameter collection lens mounted to the end of a 1000 μm core-diameter fiber optic (Ocean Optics). The collection optics were in a shielded observation room located several meters away from the explosive charge. The collection optic were aligned to view the center of each charge through a BK7 glass viewport. The collected light was sent to a time-resolved emission spectrograph constructed from a 1/8 m spectrometer (Oriel) interfaced to a 4096 pixel line-scan camera (Basler Sprint) with a data collection rate of 1–70 kHz. The resolution and usable spectral range of the spectrograph were 1.2 nm and 380–720 nm, respectively. The wavelength and intensity axes of the spectrograph were calibrated with a mercury-argon lamp (Ocean Optics) and a halogen lamp with a known color-temperature (Thorlabs), respectively. We note that due to the low light output of the color-temperature lamp in the blue region of the spectrum and the short maximum integration time of the detector (1 ms), the spectrum intensity could not be corrected for instrument response at wavelengths below ~460 nm. The spectrograph was triggered by the fire control circuits used to detonate the explosive charges. Spectra were recorded at an integration period of 15 μs per scan and each shot was repeated several times in order to confirm reproducibility.

We note that in the current investigation, detonation should be complete within ~5 μs of detonator initiation given the length of the charge and the detonation velocity of the formulation, with subsequent emission assigned to the post-detonation fireball resulting from afterburning of under-oxidized detonation products. Interestingly, spectroscopy methods similar to those used in the current study have observed very high temperatures (9700 K) associated with early ($t \leq 21$ μs) shock breakout into the surrounding air by monitoring atomic emission signals from N and O atoms.[16] We do not expect breakout effects to contribute significantly to the results of the current study on account of the longer delay times and the fact that our temperature measurements are obtained from an atom found in the explosive formulation but not in the surrounding air.

III. RESULTS AND DISCUSSION

In Figure 1, we show typical emission spectra collected from RDX charges incorporating the commercial nano-Al, AlOA, and AlFA. Each spectrum shown was collected at $t = 30$ μs, where $t = 0$ corresponds to explosion of the detonator. The spectra are remarkably similar; in each we find a broadband emission covering the entire visible spectrum, Al $^2P_{1/2} \leftarrow {}^2S_{1/2}$ and $^2P_{3/2} \leftarrow {}^2S_{1/2}$ atomic emissions at 394 and 396 nm, respectively,[19,20] and the AlO $X \leftarrow B$ vibronic band.[21] We also see a strong Na emission at 589 nm resulting from Na impurities[3] in the sample, as well as peaks at 554 nm and 706 nm due to the $^1S_0 \leftarrow {}^1P_1$ and $^3D_3 \leftarrow {}^3F_4$ transitions in Ba atoms, and peaks at 455, 493, and 614 nm from the $^2S_{1/2} \leftarrow {}^2P_{3/2}$, the $^2S_{1/2} \leftarrow {}^2P_{1/2}$, and the $^2D_{5/2} \leftarrow {}^2P_{3/2}$ transitions in Ba^+ ions, respectively.[22] The peak at 650 nm may have contributions[22] from both Ba ($^3D_3 \leftarrow {}^3D_3$) and Ba^+ ($^2D_{3/2} \leftarrow {}^2P_{1/2}$) at the resolution of the spectrograph. In the case of the charges incorporating AlOA, we also see intense Li lines at 610 nm and 671 nm, due to a Li impurity. A number of smaller unassigned peaks and bands are also found throughout the spectra. Unfortunately, no AlF vibronic bands were observed for the RDX-AlFA charges, possibly due to the weak emission character of the AlF bands found in this region of the spectrum.[21] We note that additional AlF bands have been reported[21] at wavelengths outside the spectral range of our spectrometer, and future experiments are planned to focus on any UV emissions.

Although the spectra share the same basic features, the time-dependence of the Al, AlO, and broadband emissions differs between the charges containing the various types of aluminum particles. In Figure 2, we show the intensity of the Al atomic emission and the broadband emission as measured at 600 nm as a function of time. Unfortunately, the AlO band intensities could not be readily extracted and plotted due to

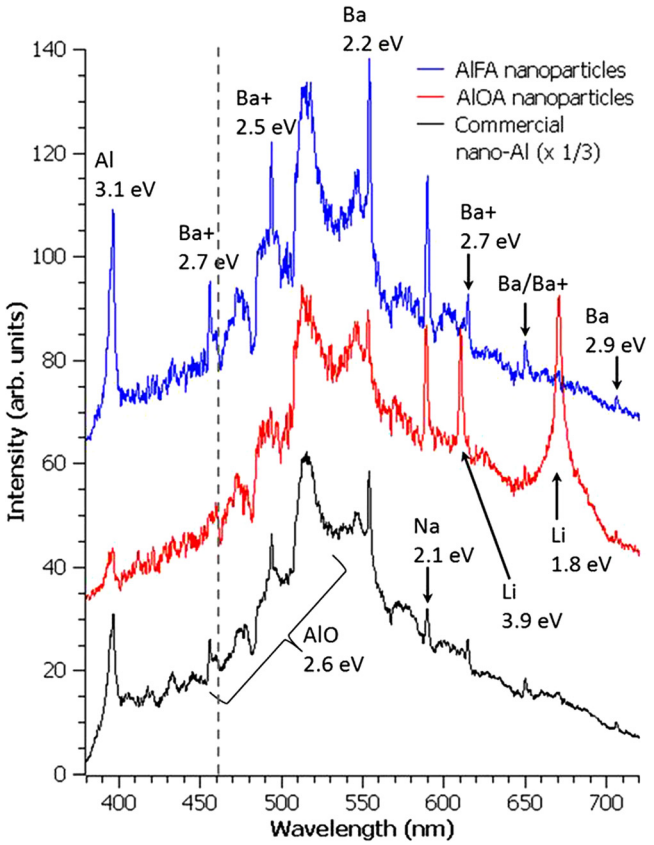

FIG. 1. Emission spectra obtained from detonation of barium-doped 20 g RDX charges containing 20 wt. % aluminum nanoparticles chosen from commercial nano-Al (bottom spectrum), AlOA (middle spectrum), or AlFA (top spectrum). All spectra were captured at $t = 30\ \mu s$ relative to the start of detonation. Prominent peaks and bands are labeled with the identity of the emitting species and the energy of the upper electronic state involved in the transition. The spectra are corrected for instrument response at wavelengths to the right of the vertical dashed line ($\lambda \geq 460$ nm).

the overlapping broadband emission in this region of the spectrum. Nevertheless, visual inspection of the spectra for the various charges as a function of time confirmed that the Al and AlO signals occurred in coincidence, as is typical during Al combustion.[23–27] In Figure 2(a), we see that for the RDX-AlOA charges, the Al atomic emission lines are strongest in the scan obtained at $t = 15\ \mu s$ and then decrease in each subsequent scan. In contrast, the RDX charges containing commercial nano-Al or AlFA exhibit little Al or AlO emission until $t = 30\ \mu s$. The time-dependence of the Al lines in these two types of charges is virtually identical. The intensity of the broadband emissions shows a similar trend. Strong broadband emissions are typically observed during Al combustion,[23–27] but we must be cautious in the interpretation of this signal since it can also be produced by particulates such as soot. In Figure 2(b), we see that the charges incorporating commercial nano-Al or AlFA again behave similarly to one another, while the evolution of the signals from the RDX-AlOA charges is shifted to somewhat earlier times. Taken at face value, the data in Figure 2 seem to indicate that combustion of the AlOA particles within the post-detonation fireball occurs on a faster timescale than either the commercial nano-Al or AlFA, and that the timescale for oxidation of the latter two particles is quite similar. If indeed this is the case, we might expect to see some evidence of this in the fireball temperatures. Temperature measurements are particularly relevant for the AlFA material, since it may be possible for the aluminum nanoparticles to react exothermically with the fluorinated acrylic matrix before competing oxidation processes can occur,[7] increasing the temperature, but producing only weak AlF vibronic signals, for example.

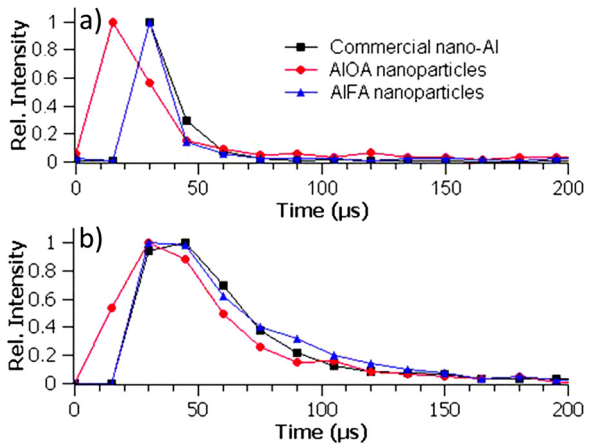

FIG. 2. Time dependence of (a) the Al atomic emission peak at 396 nm and (b) the broadband emission at 600 nm for each of the types of explosives charges studied following detonation.

In Table I, we list the apparent temperatures of the fireballs obtained from the Ba atomic emissions. The temperatures were obtained by the two-line method, utilizing the 554 and 706 nm Ba emission lines since they persisted longest following the detonations. Unfortunately, Ba emission lines were not reliably prominent in the first 1–2 scans (0, 15 μs). The error in the temperatures obtained in subsequent scans was determined by the available signal-to-noise ratio of the Ba peaks in the spectra, with higher Ba signals corresponding to lower error bars. The error bars listed in Table I correspond to either the 95% confidence level calculated from the signal-to-noise ratio of the scan or the inherent accuracy limit of the method,[28] whichever is larger. As mentioned above, each shot was repeated several times to confirm reproducibility. The temperature of the fireball resulting from the RDX charges containing the commercial nano-Al are in the range of 3600–3900 K, in good agreement with earlier measurements.[11] The temperature obtained for the RDX-AlOA charges is initially in the 4000–4500 K range, but then quickly drops to less than 2600 K for $t \geq 45\ \mu s$. We

TABLE I. Apparent fireball temperatures for the various types of explosives charges used in the current study, obtained from Ba atomic emission lines evident in the time-resolved spectra. The temperature was calculated by the two-line method using the Ba emission peaks at 554 and 706 nm. The 95% confidence levels are given in parentheses.

Time (μs)	20 wt. % commercial Al in RDX	20 wt. % AlOA in RDX	20 wt. % AlFA in RDX
0	…	…	…
15	…	4000 (400)	…
30	3900 (200)	4500 (500)	3200 (300)
45	3600 (300)	<2600	3400 (500)

can estimate only an upper bound for this temperature based upon the presence of the Ba line at 554 nm and the absence of any other Ba or Ba^+ lines in the corresponding spectrum. The temperatures obtained for the RDX-AlFA charges are in the range of 3200–3400 K. It is interesting to note that this is near the expected temperature for aluminum fluorination reactions,[29] although this may be coincidental since these particles are fuel-rich and we know from the emission spectra that oxidation is also occurring. For reference, the apparent temperatures of RDX charges that contain no Al content (obtained previously[10,11] using the same methodology) are in the range of 2600–2900 K.

We note that two Li lines from different energy levels are observed in the RDX-AlOA spectra, resulting from a Li impurity in AlOA. Unfortunately, we cannot use these to obtain an additional temperature measurement since the peak at 671 nm oversaturated the detector in the as-collected spectra (before correction for detector response was applied). The prominent pedestal at the base of this peak is most likely due to charge "bleeding" from the oversaturated pixels into neighboring ones. Additionally, the Li concentration in the sample is currently unknown, thus, we cannot be certain that the Li emissions are not subject to self-absorption effects.

The fact that the temperatures obtained for the RDX-AlOA charges is similar to (or perhaps even a bit higher than) those of the charges with commercial nano-Al, while the RDX-AlFA charges yielded lower temperatures, is consistent with the observed oxidation kinetics discussed above, i.e., that the oxidation timescales are similar for the commercial nano-Al and AlFA but that the AlOA particles burn more quickly. The AlOA and AlFA particles contain ~40 wt. % and ~50 wt. % Al metal, respectively,[5,7] only about half of the Al metal content of the commercial particles. The lower percentage of Al metal content correspondingly lowers the energy content of the explosive charge. Consequently, if the AlFA particles burn at a similar rate to the commercial nano-Al, then we would expect the temperature to be intermediate between that of RDX alone and RDX with the commercial nanoparticles. This is precisely what we observe. On the other hand, the observation that the RDX-AlOA charges are able to achieve a peak temperature at least equal to that of RDX with the commercial nanoparticles, despite the substantially lower Al content, lends additional support to the idea that the combustion kinetics for the AlOA particles are faster than those for the other particles studied. Of course, the fact that the temperature drops so quickly for the charges incorporating the AlOA particles also supports this idea.

IV. CONCLUSIONS

The results of the current investigation seem to indicate that the AlOA nanoparticles react more quickly in the fireball than either the commercial nano-Al or the AlFA nanoparticles even though the nanoparticle sizes in the samples are comparable. It also indicates that the oxidation rates of the commercial nano-Al and the AlFA particles (or at least the Al content in the AlFA material) are similar. Clearly, additional experimental investigations and possibly also input from theory will be required to establish a detailed mechanistic understanding. Nevertheless, the most straightforward interpretation of these results would seem to be that changing the passivation layer of aluminum nanoparticles from an oxide shell to organic passivation can significantly enhance the post-detonation combustion kinetics.

ACKNOWLEDGMENTS

The authors gratefully acknowledge funding and facilities provided for this work by the Air Force Research Laboratory under the NanoEnergetics Program, funding from the Air Force Office of Scientific Research (AFOSR) through the support of Dr. Michael Berman, and the financial support of the Defense Threat Reduction Agency (DTRA, Grant No. HDTRA-07-1-0026) for development of the AlOA particles. We would also like to thank Mr. Rick Beesley and Mr. Mark Grimmonpre for their assistance in conducting these experiments.

[1]P. P. Vadhe, R. B. Pawar, R. K. Sinha, S. N. Asthana, and A. S. Rao, Combust., Explos. Shock Waves **44**, 461 (2008).
[2]E. Anderson, *Tactical Missile Warheads*, Progress in Astronautics and Aeronautics Vol. 155, edited by J. Carleone (American Institute of Aeronautics and Astronautics, Washington, 1993), Chap. 2.
[3]*CRC Handbook of Chemistry and Physics*, 80th ed., edited by D. R. Lide (CRC, 2000).
[4]R. J. Jouet, A. D. Warren, D. M. Rosenberg, V. J. Bellitto, K. Park, and M. R. Zachariah, Chem. Mater. **17**, 2987 (2005).
[5]K. A. S. Fernando, M. J. Smith, B. A. Harruff, W. K. Lewis, E. A. Guliants, and C. E. Bunker, J. Phys. Chem. C **113**, 500 (2009).
[6]C. A. Crouse, C. J. Pierce, and J. E. Spowart, ACS Appl. Mater. Interfaces **2**, 2560 (2010).
[7]C. A. Crouse, C. J. Pierce, and J. E. Spowart, Combust. Flame **159**, 3199 (2012).
[8]C. E. Bunker, M. J. Smith, K. A. S. Fernando, B. A. Harruff, W. K. Lewis, J. R. Gord, E. A. Guliants, and D. K. Phelps, ACS Appl. Mater. Interfaces **2**, 11 (2010).
[9]W. K. Lewis, B. A. Harruff, J. R. Gord, A. T. Rosenberger, T. M. Sexton, E. A. Guliants, and C. E. Bunker, J. Phys. Chem. C **115**, 70 (2011).
[10]W. K. Lewis and C. G. Rumchik, J. Appl. Phys. **105**, 056104 (2009).
[11]W. K. Lewis, C. G. Rumchik, P. B. Broughton, and C. M. Lindsay, J. Appl. Phys. **111**, 014903 (2012).
[12]J. A. Orson, W. F. Bagby, and G. P. Perram, Infrared Phys. Technol. **44**, 101 (2003).
[13]J. R. Carney, J. S. Miller, J. C. Gump, and G. I. Pangilinan, Rev. Sci. Instrum. **77**, 063103 (2006).
[14]J. Wilkinson, J. M. Lightstone, C. J. Boswell, and J. R. Carney, in *Shock Compression of Condensed Matter*, edited by M. Elert, M. D. Furnish, R. Chau, N. Homes, and J. Nguyen (American Institute of Physics, 2007), p. 1271.
[15]K. C. Gross, J. Wayman, and G. P. Perram, Proc. SPIE **6566**, 656613 (2007).
[16]J. D. Koch, S. Piecuch, J. M. Lightstone, J. R. Carney, and J. Hooper, J. Appl. Phys. **108**, 036101 (2010).
[17]V. Bouyer, G. Baudin, C. Le Gallic, and P. Hervé, in *Shock Compression of Condensed Matter*, edited by M. D. Furnish, N. N. Thadhani, and Y. Horie (American Institute of Physics, 2001), p. 1223.
[18]V. Bouyer, I. Darbord, P. Hervé, G. Baudin, C. Le Gallic, F. Clément, and G. Chavent, Combust. Flame **144**, 139 (2006).
[19]K. B. S. Eriksson and H. B. S. Isberg, Ark. Fys. **23**, 527 (1963).
[20]C. Mendoza, W. Eissner, M. Le Dourneuf, and C. J. Zeippen, J. Phys. B **28**, 3485 (1995).
[21]R. W. B. Pearse and A. G. Gaydon, *The Identification of Molecular Spectra* (Chapman & Hall, 1963).
[22]J. J. Curry, J. Phys. Chem. Ref. Data **33**, 725 (2004).
[23]J. L. Gole and R. N. Zare, J. Chem. Phys. **57**, 5331–5335 (1972).

[24]S. Rosenwaks, R. E. Steele, and H. P. Broida, J. Chem. Phys. **63**, 1963–1965 (1975).
[25]S. Goroshin, J. Mamen, A. Higgins, T. Bazyn, N. Glumac, and H. Krier, Proc. Combust. Inst. **31**, 2011–2019 (2007).
[26]M. Jackson, M. Pantoya, and W. Gill, Combust. Flame **153**, 58–70 (2008).
[27]P. E. Bocanegra, D. Davidenko, V. Sarou-Kanian, C. Chauveau, and I. Gökalp, Exp. Therm. Fluid Sci. **34**, 299–307 (2010).
[28]I. Reif, V. A. Fassel, and R. N. Kniseley, Spectrochim. Acta, Part B **29**, 79 (1974).
[29]C. D. Yarrington, S. F. Son, and T. J. Foley, J. Propul. Power **26**, 734 (2010).